The Astrophysical Journal, 862:90 (7pp), 2018 July 20 https://doi.org/10.3847/1538-4357/aace5d


# The Revolution Revolution: Magnetic Morphology Driven Spin-down*

C. Garraffo[1], J. J. Drake[1], A. Dotter[1], J. Choi[1], D. J. Burke[1], S. P. Moschou[1], J. D. Alvarado-Gómez[1], V. L. Kashyap[1], and O. Cohen[1,2]
[1] Harvard-Smithsonian Center for Astrophysics, 60 Garden Street Cambridge, MA 02138, USA
[2] Lowell Center for Space Science and Technology, University of Massachusetts Lowell, 600 Suffolk Street, Lowell, MA 01854, USA
*Received 2018 April 5; revised 2018 May 29; accepted 2018 June 14; published 2018 July 25*

## Abstract

Observations of young open clusters (OCs) show a bimodal distribution of rotation periods that has been difficult to explain with existing stellar spin-down models. Detailed magnetohydrodynamic (MHD) stellar wind simulations have demonstrated that surface magnetic field morphology has a strong influence on wind-driven angular momentum loss. Observations suggest that faster rotating stars store a larger fraction of their magnetic flux in higher-order multipolar components of the magnetic field. In this work, we present an entirely predictive new model for stellar spin-down that accounts for the stellar surface magnetic field configuration. We show how a magnetic complexity that evolves from complex toward simple configurations as a star spins down can explain the salient features of stellar rotation evolution, including the bimodal distribution of both slow and fast rotators seen in young OCs.

*Key words:* stars: activity – stars: evolution – stars: rotation

## 1. Introduction

The rotation evolution of stars has been extensively studied over the last five decades but remains one of the most challenging and open problems in stellar astrophysics. Rotation is relevant for stellar evolution itself, for stellar age determination via the technique of "gyrochronology" (Skumanich 1972; Soderblom 1983; Barnes 2003; Meibom et al. 2015), and is the driver of stellar magnetic activity. The growing realization that the latter plays a crucial role in exoplanet detection (see, for example, Hatzes 2013a, 2013b, 2016; Donati et al. 2016) and on exoplanet atmospheric evolution and habitability (Sanz-Forcada et al. 2011; Lammer et al. 2012; Chadney et al. 2016, 2017; Garraffo et al. 2016a, 2017; Cohen et al. 2018), combined with the increasing number of precise measurements of the rotation periods of stars, presents a renewed motivation to revise our understanding of stellar rotation.

Magnetic braking is the dominant mechanism by which Sun-like and later-type stars spin-down, and it is determined by the magnetic fields on their surfaces (Weber & Davis 1967; Kawaler 1988). Stellar rotation fuels magnetic activity through dynamo action and, in turn, activity controls spin-down rates. This self-regulating mechanism results in a relationship between the rotation period and mass that evolves with time. Observations of open clusters (OCs) of known ages indeed show stars for which rotation angular velocities ($\Omega$) follow the Skumanich spin-down law, $\Omega \sim t^{-1/2}$, but they also show persistent fast rotators whose origin remains a mystery.

The implication of the observations is that some stars undergo a fairly rapid spin-down whereas others of the same mass and age do not. A considerable amount of recent theoretical work has been aimed at explaining this OC rotational bimodality. One of the first empirical models is the double zone model (see Spada et al. 2011, and references therein) and recent variations of it (Reiners & Mohanty 2012; Gallet & Bouvier 2013). This model is based on the analytical prescription for the stellar wind torque given by Kawaler (1988) and includes a bifurcation at a certain critical stellar rotation frequency $\Omega_{\rm crit}$.

The symmetrical empirical model of Barnes (2010) and Barnes & Kim (2010) also uses a bifurcated prescription for the torque, and is based on the idea of a sudden coupling of the stellar radiative core with its convective envelope that results in a fast and dramatic spin-down due to the sudden change in moment of inertia. The latter has been the standard solution until recently, when the same bimodal behavior was observed for fully convective stars (Douglas et al. 2016, 2017; Newton et al. 2016), suggesting that the radiative core does not play a significant role in the sudden change of angular velocity.

Recent studies have aimed for a more unified scenario. While great progress has been made with sophisticated, physics-based, and realistic models (Matt et al. 2012, 2015; Pantolmos & Matt 2017; Sadeghi Ardestani et al. 2017), these still do not recover the bimodal morphology of the color-period diagram. Johnstone et al. (2015) successfully modeled the spread in rotation rates but only partially recovered the bimodality of their distributions as reflection of a bifurcated wind torque formula. Qureshi et al. (2018) recently did a proof-of-concept calculation that shows planet consumption by a star can lead to faster rotation.

Brown (2014) presented the first prescription that successfully reproduces the simultaneous presence of rapid and slow branches, and the sparsely populated gap between them, and matches observations reasonably well. This metastable dynamo model (MDM) is based on the idea that rotating stars fall into two different regimes, one in which the dynamo is strongly coupled to the wind, which accounts for the Skumanich branch, and the other one in which it is weakly coupled and gives rise to the branch of fast rotators. MDM requires a spontaneous and random change of mode from the former to the latter, with a mass-dependent transition probability, and predicts that the angular momentum loss (AML) efficiency in the strongly coupled regime is at least two orders of magnitude larger than that in the weakly coupled regime. However, this model lacks a

* Title inspired by C. L. Davis PhD Thesis *Revolution evolution: tracing angular momentum during star and planetary system formation*, St. Andrews University.

physical basis for each regime and a mechanism for the transition between them.

All existing models for stellar spin-down have, to a large extent, neglected the geometry of stellar surface magnetic fields. An increasing number of Zeeman–Doppler-Imaging (ZDI) observations indicate that young, active stars store a larger fraction of their magnetic flux in higher-order multipole components of the magnetic field, i.e., complex field configurations (e.g., Donati 2003; Donati & Landstreet 2009; Marsden et al. 2011; Alvarado-Gómez et al. 2015; Waite et al. 2015). What effects this may have on spin-down rates is, then, of considerable interest and has been the subject of a handful of recent studies (Garraffo et al. 2015, 2016b; Réville et al. 2015).

Garraffo et al. (2015) have shown that the complexity of the large-scale magnetic field can dramatically reduce the AML rates by a few orders of magnitude. As a consequence, one should expect their magnetic braking efficiency to be lower than that of their slower rotating relatives. Garraffo et al. (2015) pointed out that this complexity provides a physical basis for the MDM model and, therefore, might naturally explain the bimodal distribution of rotation periods observed in OCs. Garraffo et al. (2016b, hereafter CG16) quantified this effect, providing scaling laws for stellar angular momentum loss rates as a function of complexity together with a prescription for applying them to real stars. Later, Finley & Matt (2017, 2018) and See et al. (2018) used scaling laws based on a set of thermally driven polytropic wind simulations to explore the effect of mixed modes.

Recently, van Saders et al. (2016) reported an additional later deviation from standard gyrochronology. They find that after stars reach a Rossby number $\sim 2$ ($Ro = P/\tau$, where $\tau$ is convective turnover time), they rotate faster than expected from the Skumanich law and, therefore, appear to be losing angular momentum less efficiently. This, together with a reported deficit of observed rotation periods longer than the Sun among solar type stars (see van Saders et al. 2018, and references therein), suggest that a very efficient magnetic braking suppression takes place at later ages. This could be due to a sudden decrease in magnetic field strength, but it would require a very dramatic change in the dynamo. Instead, it can be explained by a smooth increase in magnetic field complexity at late times that, given the steep dependency of angular momentum loss efficiency with complexity, would result in a sharp magnetic braking suppression.

In this work, we present a new prescription for the rotation evolution of young, active stars that includes the modulation of spin-down rates derived by CG16. We confirm that accounting for magnetic complexity in our spin-down models results in the bimodal distribution observed in OCs and its observed evolution over time.

This paper is organized as follows. In Section 2 we describe the spin-down model, in Section 3 we detail the method we used to generate population synthesis, in Section 4 we describe the observations against which we will compare our populations, and in Sections 5 and 6 we discuss our results and their implications. Lastly, in Section 7, we summarize our conclusions.

## 2. The Model

Weber & Davis (1967) provided the first prescription for calculating angular momentum loss rates. Their model assumed spherical symmetry and was later generalized by simple scaling relations (Kawaler 1988; Krishnamurthi et al. 1997). Observations support the idea that the slow rotator branch follows the Skumanich spin-down law, $P \sim t^{1/2}$, where $P$ is the rotation period of the star, and, therefore, rotation periods can be determined as a function of stellar mass and age.

Our prescription for angular momentum loss rates is based on two assumptions. The first assumption is that stars with a dominant dipolar component of the magnetic field follow a Skumanich spin-down law with a mass dependence that reflects the convective turnover time, $\tau$. The latter is currently a standard assumption, based on theoretical work by Durney & Latour (1978), for all stars regardless of their magnetic field configuration (see, for example, Barnes 2003; Barnes & Kim 2010; Brown 2014). The second assumption is that the magnetic fields of fast rotating stars have more complex large-scale geometries, which, as discussed before, is supported by ZDI observations. Magnetic complexity is expected to reduce the angular momentum loss rates significantly (Garraffo et al. 2015; Réville et al. 2015) and we employ the scaling laws derived by CG16. The model presented here then uses a simple magnetic braking prescription based on a Skumanich spin-down law together with this magnetic complexity modulation.

The angular momentum loss can be written as

$$\dot{J} = \dot{J}_{\rm Dip} Q_J(n), \tag{1}$$

where $\dot{J}_{\rm Dip}$ represents the dipolar losses and $Q_J(n)$ is a modulating factor that accounts for the complexity of the magnetic fields on the stellar surface, parametrized by $n$ (see CG16 for details). The dipolar branch, which corresponds to $Q_J = 1$, evolves in time following a Skumanich law, $P_{\rm Dip} \sim t^{0.5}$, that translates into the angular momentum loss rate as

$$\dot{J}_{\rm Dip} = c \cdot \Omega^3 \tau, \tag{2}$$

where $c$ is a normalization factor related to the wind efficiency for a dipole, and is well-constrained by observations and stellar spin-down timescales. The shape of this branch reflects the color dependence of the convective turnover time $\tau$. We use the magnetic complexity modulation factor derived by CG16,

$$Q_J(n) = 4.05\, e^{-1.4n} + (n-1)/(60B \cdot n), \tag{3}$$

where $n$ is the complexity of the magnetic field ($n = 1$ represents a dipole and is larger for higher complexity) and $B$ represents the magnetic field strength. The second term becomes important only for $n > 7$, at which the spin-down rate reaches a plateau (see Figure 3 from CG16). We neglect this effect by imposing $n = 7$ as the maximum complexity and, therefore, the above equation simplifies to

$$Q_J(n) = 4.05\, e^{-1.4n}. \tag{4}$$

As discussed earlier, according to ZDI observations, young, fast rotating stars seem to be more complex and, therefore, we expect $n$ to decrease with the rotation period or its dimensionless relative Rossby number, $Ro = P_{\rm rot}/\tau$. On the other hand, recent *Kepler* observations show a deviation from gyrochronology at $Ro \sim 1$–$2$ , that in this scenario corresponds to a new increase of complexity. We propose a simple function for the complexity of the magnetic field with a Rossby number (see Figure 1) that reflects the trends suggested by these

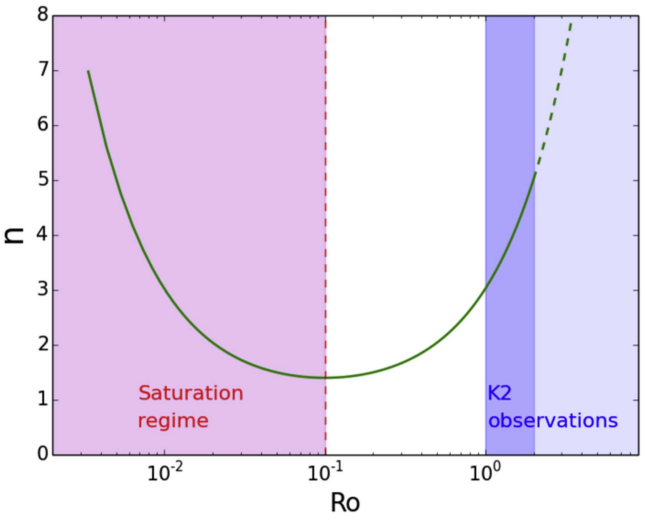


**Figure 1.** Proposed complexity of the magnetic field as a function of the Rossby number consistent with OC and *K2* observations. The pink shaded area represents the saturated regime observed in X-rays and the blue shaded area represents the Rossby numbers at which the later deviation from gyrochronology is observed.

observations,

$$n = \frac{a}{Ro} + 1 + bRo, \tag{5}$$

where $a = 0.02$ and $b = 2$ are the free parameters in our model and were determined using OC observations. The first term represents the decrease in complexity with the rotation period for young, fast rotating stars, suggested by the ZDI observations. The constant 1 is just reflecting the fact that the minimum possible complexity is a pure dipole and has been defined as $n = 1$ by CG16. The minimum of this function has been taken to be slightly higher than one given that even the stars on the slow rotator branch, expected to follow Skumanich, are probably not perfect dipoles. The third term is included to represent the increase in complexity at later times that would explain the *Kepler* observations and it only becomes important at larger Rossby numbers than the ones most relevant for this work. We emphasize that this term is not necessary for the success of our model in reproducing the young stellar cluster observations shown here. It will, however, make a difference when modeling older cluster rotation period distributions.

Under this description, the angular momentum loss rate for any given star is a function of just its Rossby number. In Figure 2, we have reproduced the rotation evolution of a solar mass star starting at 13 Myr (immediate post-disk phase) for different initial conditions with and without considering the magnetic modulation of the angular momentum loss efficiency.

## 3. Population Synthesis

To compare our model with OC observations, we generate a population of stars with initial rotation periods and stellar masses from the h Persei Cluster (Moraux et al. 2013; see Figure 3).

We use Monte Carlo simulations with a time step of $10^4$ yr and evolve the population for 1 Gyr. We include the evolution of each star's mass, radius, moment of inertia, and effective temperature using the *MIST* evolutionary tracks (Paxton et al. 2011, 2013, 2015; Dotter 2016). We do not use the rotation periods from the *MIST* tables, instead, the rotation periods are self-consistently evolved according to our model. At each step we compute the spin-up or down that results from the contraction or expansion, and consequent moment of inertia change, of the star in order to conserve angular momentum, and the spin-down that results from the loss of angular momentum through winds using the magnetic braking prescription from Section 2, assuming solid-body rotation. To do so we calculate the Rossby number using convective turnover times from the *MIST* models and derive the magnetic complexity of each star using Equation (5), and its angular momentum loss rate using Equations (2) and (4). The new rotation period is then computed.

Stars are born with a circumstellar disk that lasts for up to a few Myr and is expected to prevent them from spinning up as they contract through disk locking (Rebull et al. 2002, 2004). By ~10 Myr, all starts have lost their disks (which corresponds to the birth line of Stahler (1983) and Palla & Stahler (1990) at the end of the disk-locking time). Our model is not very sensitive to the assumed initial conditions or the duration of disk locking. For the results presented here, we start our rotation evolution in the immediate post-disk phase in order to avoid introducing extra free parameters related to disk locking, as pointed out by Rebull et al. (2018). We use as our starting conditions the rotation periods of stars in the 13-Myr-old cluster h Persei. We have tested the rotation evolution outcomes using different initial distributions, for example the rotation periods of stars in the Orion Nebula Cluster with disk locking, as well as an homogeneous distribution of masses (0.3–1.6 $M_\odot$) and periods (0–15 days). We find that the initial conditions are largely erased fairly quickly (<200 Myr) and we recover the same bimodal distribution of the rotation periods. The reason for this can be seen in Figure 2. The initial period of each star will only determine how long that particular star will remain in the branch of fast rotators. Shorter disk-locking times will result in stars spinning up over a longer time interval and, therefore, should lead to more stars in the bottom branch at early ages (~100 Myr). But the general bimodal distribution of rotation periods will be, overall, unaffected.

We fix the normalization constant related to dipolar angular momentum losses to $c = 1 \times 10^{41}$ gm cm$^2$, which provides the best fit to the Skumanich branch in OC observations. This is consistent with a reasonable solar angular momentum loss rate of $\dot{J}_{\rm Dip} \sim \times 10^{30}$ gm cm$^2$ s$^{-2}$ (Pognan et al. 2018) as becomes clear from Figure 2.

For each star, there is an intrinsic maximum velocity at which centrifugal forces exceed self-gravity, called the break-up velocity, that is a function of $M$ and $R$,

$$\Omega_{\rm break\text{-}up} = \sqrt{\frac{GM}{R^3}},$$

where $G$ is Newton's constant, and $M$ and $R$ are the star's mass and radius, respectively. We assume stars are solid-body rotators and impose this limit in order to have a physically consistent model. This does not qualitatively affect our results.

We chose a sample of stars large enough to get a reliable probability density for each rotation period as a function of color and age. For visualization we use a smaller group of 600 stars, comparable to the number of stars in each observation.

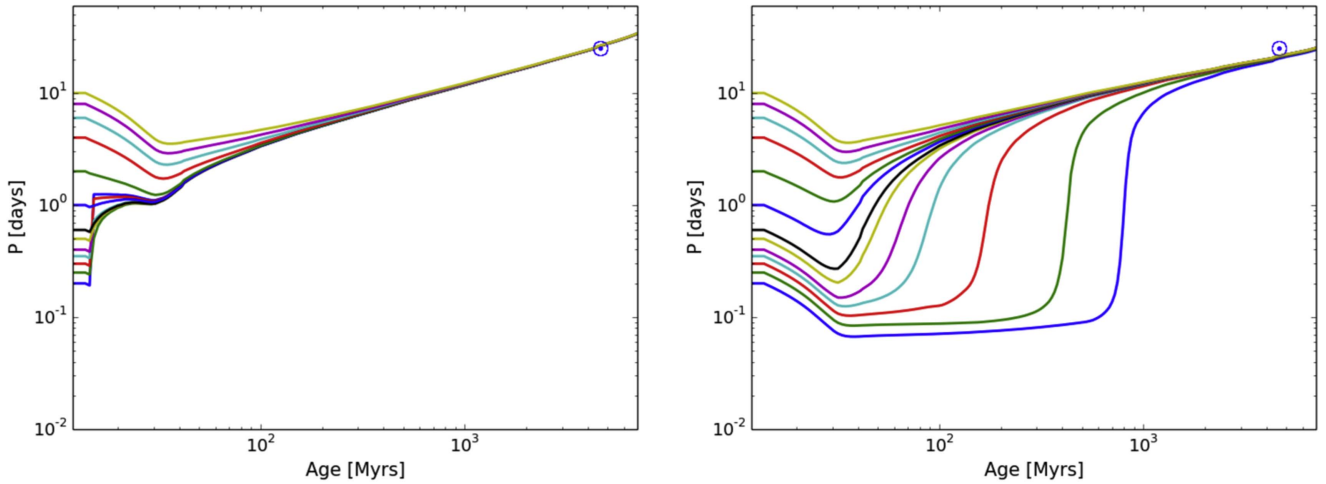


**Figure 2.** Rotation period evolution of a solar mass star for different initial periods. The left panel shows evolution without taking into account the complexity modulation (Skumanich-like spin-down), and the right panel shows the same but including the complexity modulation, which corresponds to our model predictions. In both panels the present-day Sun is indicated.

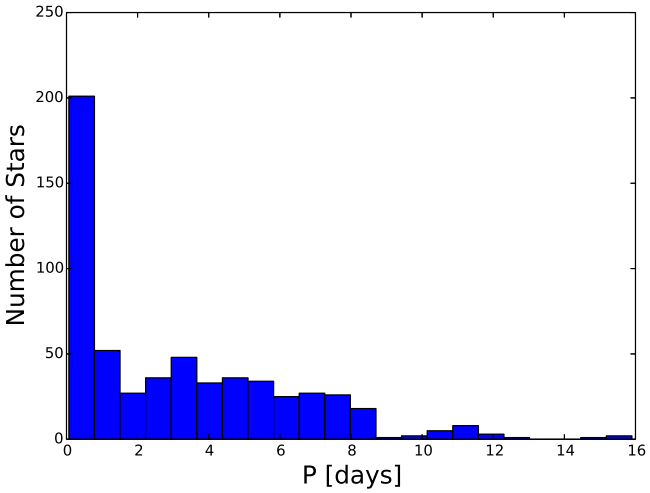


**Figure 3.** Histogram of initial periods from h Persei Cluster.

## 4. OC Observations

We compare our predictions to rotation period observations for stars of different ages, ranging from 50 Myr to 1 Gyr. By doing so we can judge the performance of our model both in terms of reproducing the bimodal period distributions of the observations as well as their time evolution. We use the rotation periods and ages from the following clusters available in the literature: Pleiades ∼70–150 Myr (Hartman et al. 2010; Rebull et al. 2016), Hyades ∼500–625 Myr (Radick et al. 1987; Delorme et al. 2011; Douglas et al. 2016), Coma ∼500 Myr (Radick et al. 1990), M34 ∼ 200–250 Myr (Barnes 2003; Meibom et al. 2011b), M35 ∼100–150 Myr (Meibom et al. 2009), M37 ∼ 346–550 Myr (Hartman et al. 2009; Wu et al. 2009), Praesepe ∼550–700 Myr (Delorme et al. 2011; Douglas et al. 2017; Rebull et al. 2017), and NGC 6811 ∼1 Gyr (Meibom et al. 2011a). We compare predicted and observed periods versus $B - V$ color, converting $V - Ks$ colors to $B - V$ using the tables by Pecaut et al. (2012) where necessary.

## 5. Results

We have compared Skumanich-like rotation evolution with the one predicted by our model for each stellar mass (we show only the one solar mass case in Figure 2). In the former, the absence of the complexity-induced weakening of angular momentum loss in the T Tauri phase means that wind-driven spin-down dominates over contraction-driven spin-up for the fastest initial rotators, such that those stars never achieve more rapid rotation than at their immediate post-disk phase: all converge to a rotation period of approximately 1 day at an age of 15 Myr.

In our model, stars that have shorter initial rotation periods remain fast rotating for longer, until they undergo a sharp spin-down process at an age that depends on their mass and initial period (see Figure 2). The spread in the transition time is larger for lower mass stars, which explains why more massive stars transition first and why a bimodal distribution of the rotation periods is observed for late spectral types in older clusters. At constant ages between a few tens of Myr and up to a few hundred Myr, we can see a concentration of stars at a long period and a short period (right panel of Figure 2), and a few stars in between, which is the basis for bimodality.

In Figure 4, we compare population synthesis generated with our model (predicted density of stars in blue) to OC observations (observed stars in red). For each age, we combine all available observations. We find, as expected from the solar mass star rotation evolution just discussed, that the bimodal distribution of rotation periods observed in OCs naturally arises (see Figure 4), as do other characteristics of the rotation period distributions. The fast rotator branch near the bottom of each panel gets less populated with age, while the Skumanich top branch becomes more populated; stars with higher masses transition first. In addition, we recover the mass dependence of the Skumanich branch.

## 6. Discussion

We find that including the magnetic modulation of angular momentum loss rates predicted from simulations (CG16) together with the complexity evolution observed by ZDI results in the bimodal rotation morphology observed in OCs. By proposing a well-motivated complexity evolution function, we obtain good agreement for both branches, the gap between them, their mass dependency, and the time evolution of all of the ingredients.

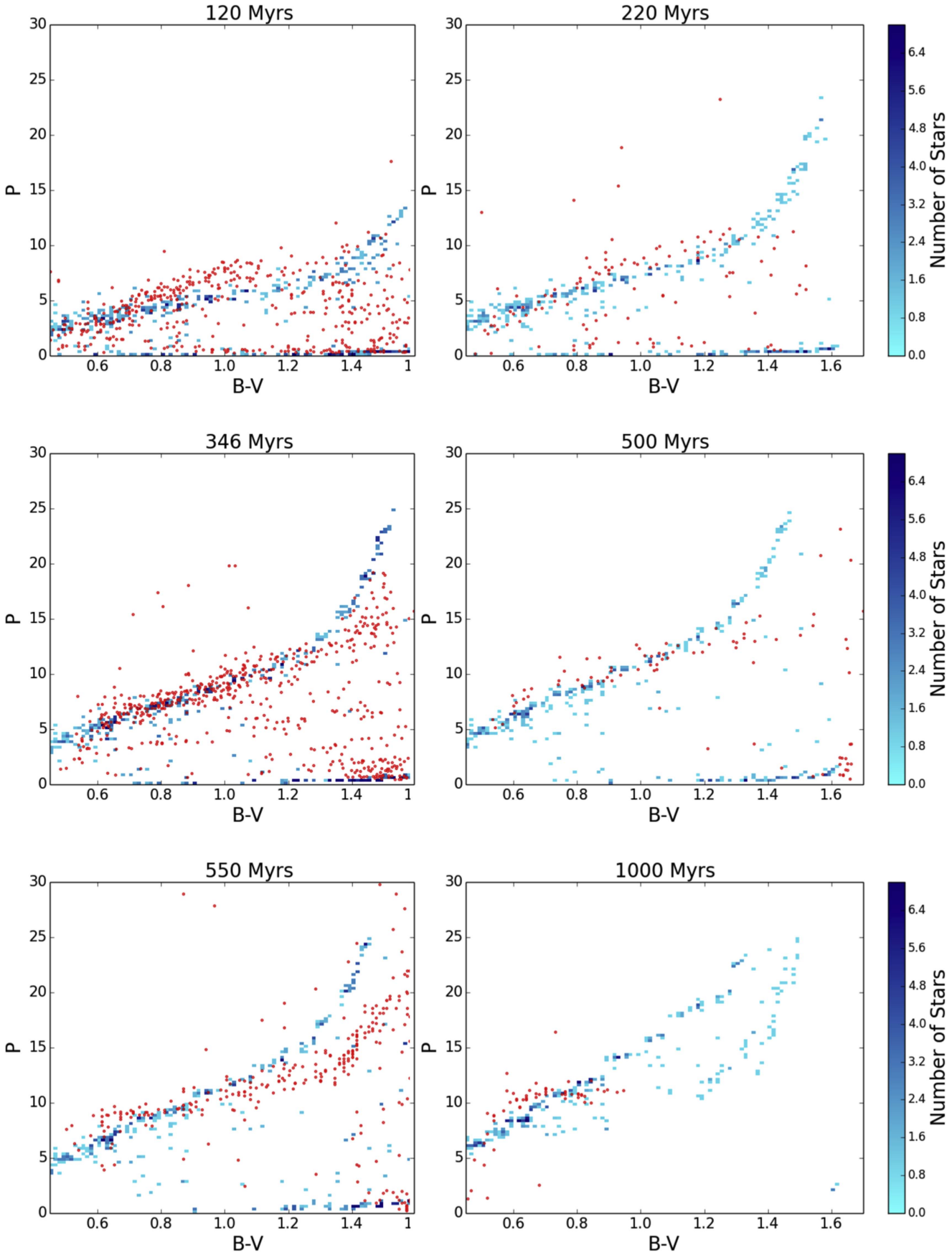


**Figure 4.** Rotation periods as a function of $B - V$ color observed in OCs of increasing age (from top left to bottom right) are in red. In blue we show the probability density predicted by our model for each OC age (the color bar represents number of stars). We normalized our prediction to reflect the number of counts observed in each color bin.

In this scenario, stars are magnetically more complex for Rossby numbers <0.1. Interestingly, this corresponds to the saturation regime (see, for example, Wright et al. (2011), and references therein) in which X-ray emission reaches a plateau and faster rotation no longer results in stronger emission. Our results suggest that stars are magnetically complex in the saturated regime and become simpler by the time they reach $Ro = 0.1$, when they exit saturation and begin losing angular momentum efficiently. In this picture, complexity is only determined by the Rossby number. Higher mass stars with shorter convective turnover times, and consequently higher Rossby numbers for a given rotation period, transition sooner to the Skumanich branch.

While the model presented here was originally motivated by the MDM model of Brown (2014), it has one important difference. Rotation evolution in the magnetic complexity driven spin-down model is entirely predictive from the moment of the alleviation of disk locking. At this time, its future rotation trajectory is determined entirely by its initial rotation period. MDM includes an unavoidably stochastic component. While the physical mechanism responsible for the magnetic braking change is not specified, a discontinuous change in complexity that would cause a rapid change in rotation period would be a possibility. In such a scenario, stars within the gap between the rapid rotators and the Skumanich branch should all have similar (low) magnetic complexity. Instead, the model presented here implies continuous evolution of the magnetic complexity at the stellar surface, determined by the star's Rossby number, that results in a smooth (although steep) decrease in the rotation period. The increasing number of ZDI observations should eventually help us distinguish between the two theories by showing whether or not a tight complexity/rotation relationship exists for these stars.

### 6.1. Deviations from the Skumanich Law and Uncertainties in Cluster Ages

Slight deviations from the Skumanich law have been discussed in the literature (see, for example Johnstone et al. (2015); Gallet & Bouvier (2015), and references therein). Brown (2014), for example, noted that no single function of color provides a good fit to all of the OC observations and, therefore, includes a correction to the Skumanich law that depends on the cluster's age. We find the same problem here when assuming stars evolve as predicted by the Skumanich law. This can be seen from the discrepancy of the slow rotator branch (Figure 4), especially for lower mass stars ($B-V>1$). However, our main aim here is to understand the origin of the bimodal aspect of observed rotation periods and we therefore employ the standard Skumanich prescription and defer treatment of these additional details to future work.

There is some uncertainty in the reported ages of these clusters (see Section 4) that might lead to discrepancies with our model predictions. Further discussion of these is beyond the scope of the present paper, though we note that errors in ages will mainly affect the time evolution of the Skumanich branch. We emphasize that the strength of the model presented here is that it qualitatively reproduces the morphology of the observations, provides a physics-based explanation, and predicts the existence of the fast rotator branch and the unpopulated gap in between the two branches. In terms of our model, a change in cluster age could be accounted for in an overall shift of the apparent complexity function, $n$, with a Rossby number and our conclusions would not be affected.

### 6.2. Potential Complications from Binaries

Binary systems represent a large fraction (∼27%) of the stellar population and it are important to consider if their spin-down process is different than that of a single star. While Bouvier et al. (1997) found no difference in rotation speeds between single and binary stars in the Pleiades (∼120 Myr), Patience et al. (2002) reported that binaries with small separations (10–60 au) rotate faster than wider binaries in $\alpha$ Persei (∼60 Myr). Later, Meibom et al. (2007) found that binary stars rotate faster, on average, than single stars in M35 (∼150 Myr).

Binary companions might affect spin-down rates of the system via tidal effects, magnetic interaction, or by altering the conditions of star formation or protoplanetary disk dispersal. The gravitational and magnetic effects are only relevant for close binary systems and, while they can be significant in terms of spin-down rates (e.g., Zahn 1977; Hut 1981; Cohen et al. 2012), these systems make up only a small percentage of total cluster populations (e.g., Meibom et al. 2007) and we do not consider them further.

A wider binary companion could still affect the rotation velocity of the system by truncating the disk that is thought responsible for preventing the star from spinning up at early stages through disk locking (Lin et al. 1993; Artymowicz & Lubow 1994; Armitage & Clarke 1996). This would be expected to result in binary systems having, on average, shorter rotation periods at early ages and is consistent with the observations of young clusters. Magnetic braking, however, introduces a self-regulating mechanism by which faster rotators spin-down faster and by a few Myr this effect should be erased. Thus, in the absence of any other mechanisms, we should not expect wide binaries to have a different rotation evolutionary path than single stars. Our model offers a new explanation for these observations. If binary stars have, on average, shorter periods at early ages, that should result in them transitioning systematically later to the Skumanich branch (see Figure 2). More observations of the rotation periods of binary systems with a range of different ages and masses would be useful to confirm this.

Lastly, metallicity might affect spin-down rates through the envelope opacity that determines the depth of the convection zone and, therefore, the convective turnover time, $\tau$. In our model, the efficiency of the angular momentum mass loss rates is regulated by the Rossby number and, through it, $\tau$ has a role in determining the complexity of the stellar surface magnetic fields. While this should be taken into account when modeling stellar spin-down in general, the OCs used here all have metallicities, Fe/H, within ±0.16 of the solar value (Mermilliod et al. 1997; Stauffer 1997; Pinsonneault et al. 2004). We neglect the effects of metallicity in our model for the present, though it might become more relevant in future work when extending rotation evolution models to older populations.

## 7. Conclusions

We have presented a spin-down model that, for the first time, accounts for the morphology of the stellar surface magnetic field. Modulation of angular momentum loss according to the magnetic field complexity based on detailed MHD simulations has been included in the evolution of solid-body rotation. Spin-

down that follows a Skumanich law can explain observed bimodal OC rotation periods by including a magnetic complexity that decreases with stellar rotation period, as indicated by surface magnetic field observations. The model is entirely predictive from the moment a star loses its proto-planetary disk in the T Tauri phase and its rotation evolution is governed by its change in moment of inertia and wind-driven angular momentum loss.

We thank the anonymous referee for very constructive comments. C.G. thanks Steven Saar, Soren Meibom, Stephanie Douglas, Ruth Angus, Scott Wolk, and Sean Matt for helpful comments and discussion. C.G. was supported by *Chandra* grants GO7-18017X and GO5-16021X. J.J.D., V.L.K., and D.J.B. were supported by NASA contract NAS8-03060 to the *Chandra* X-ray Center. J.D.A.G. was supported by *Chandra* grants AR4-15000X and GO5-16021X. S.P.M. and O.C. were supported by NASA Living with a Star grant number NNX16AC11G. Numerical simulations were performed on the NASA HEC Pleiades system under award SMD-13-4526.

## ORCID iDs

C. Garraffo https://orcid.org/0000-0002-8791-6286
J. J. Drake https://orcid.org/0000-0002-0210-2276
A. Dotter https://orcid.org/0000-0002-4442-5700
J. Choi https://orcid.org/0000-0002-8822-1355
D. J. Burke https://orcid.org/0000-0003-4428-7835
S. P. Moschou https://orcid.org/0000-0002-2470-2109
J. D. Alvarado-Gómez https://orcid.org/0000-0001-5052-3473
V. L. Kashyap https://orcid.org/0000-0002-3869-7996
O. Cohen https://orcid.org/0000-0003-3721-0215

## References

Alvarado-Gómez, J. D., Hussain, G. A. J., Grunhut, J., et al. 2015, A&A, 582, A38
Armitage, P. J., & Clarke, C. J. 1996, MNRAS, 280, 458
Artymowicz, P., & Lubow, S. H. 1994, ApJ, 421, 651
Barnes, S. A. 2003, ApJ, 586, 464
Barnes, S. A. 2010, ApJ, 722, 222
Barnes, S. A., & Kim, Y.-C. 2010, ApJ, 721, 675
Bouvier, J., Rigaut, F., & Nadeau, D. 1997, A&A, 323, 139
Brown, T. M. 2014, ApJ, 789, 101
Chadney, J. M., Galand, M., Koskinen, T. T., et al. 2016, A&A, 587, A87
Chadney, J. M., Koskinen, T. T., Galand, M., Unruh, Y. C., & Sanz-Forcada, J. 2017, A&A, 608, A75
Cohen, O., Drake, J. J., & Kashyap, V. L. 2012, ApJL, 746, L3
Cohen, O., Glocer, A., Garraffo, C., Drake, J. J., & Bell, J. M. 2018, ApJL, 856, L11
Delorme, P., Collier Cameron, A., Hebb, L., et al. 2011, MNRAS, 413, 2218
Donati, J.-F. 2003, in EAS Publications Ser. 9, Magnetism and Activity of the Sun and Stars, ed. J. Arnaud & N. Meunier (Les Ulis: EDP), 169
Donati, J.-F., & Landstreet, J. D. 2009, ARA&A, 47, 333
Donati, J. F., Moutou, C., Malo, L., et al. 2016, Natur, 534, 662
Dotter, A. 2016, ApJS, 222, 8
Douglas, S. T., Agüeros, M. A., Covey, K. R., et al. 2016, ApJ, 822, 47
Douglas, S. T., Agueros, M. A., Covey, K. R., et al. 2017, yCat, 179
Durney, B. R., & Latour, J. 1978, GApFD, 9, 241
Finley, A. J., & Matt, S. P. 2017, ApJ, 845, 46
Finley, A. J., & Matt, S. P. 2018, ApJ, 854, 78
Gallet, F., & Bouvier, J. 2013, A&A, 556, A36
Gallet, F., & Bouvier, J. 2015, A&A, 577, A98
Garraffo, C., Drake, J. J., & Cohen, O. 2015, ApJ, 813, 40
Garraffo, C., Drake, J. J., & Cohen, O. 2016a, ApJL, 833, L4
Garraffo, C., Drake, J. J., & Cohen, O. 2016b, A&A, 595, A110
Garraffo, C., Drake, J. J., Cohen, O., Alvarado-Gómez, J. D., & Moschou, S. P. 2017, ApJL, 843, L33
Hartman, J. D., Gaudi, B. S., Holman, M. J., et al. 2009, ApJ, 695, 336
Hartman, J. D., Bakos, G. Á, Kovács, G., & Noyes, R. W. 2010, MNRAS, 408, 475
Hatzes, A. P. 2013a, ApJ, 770, 133
Hatzes, A. P. 2013b, AN, 334, 616
Hatzes, A. P. 2016, A&A, 585, A144
Hut, P. 1981, A&A, 99, 126
Johnstone, C. P., Güdel, M., Brott, I., & Lüftinger, T. 2015, A&A, 577, A28
Kawaler, S. D. 1988, ApJ, 333, 236
Krishnamurthi, A., Pinsonneault, M. H., Barnes, S., & Sofia, S. 1997, ApJ, 480, 303
Lammer, H., Güdel, M., Kulikov, Y., et al. 2012, EP&S, 64, 179
Lin, D. N. C., Papaloizou, J. C. B., & Kley, W. 1993, ApJ, 416, 689
Marsden, S. C., Jardine, M. M., Ramírez Vélez, J. C., et al. 2011, MNRAS, 413, 1922
Matt, S. P., Brun, A. S., Baraffe, I., Bouvier, J., & Chabrier, G. 2015, ApJL, 799, L23
Matt, S. P., MacGregor, K. B., Pinsonneault, M. H., & Greene, T. P. 2012, ApJL, 754, L26
Meibom, S., Barnes, S. A., Latham, D. W., et al. 2011a, ApJL, 733, L9
Meibom, S., Barnes, S. A., Platais, I., et al. 2015, Natur, 517, 589
Meibom, S., Mathieu, R. D., & Stassun, K. G. 2007, ApJL, 665, L155
Meibom, S., Mathieu, R. D., & Stassun, K. G. 2009, ApJ, 695, 679
Meibom, S., Mathieu, R. D., Stassun, K. G., Liebesny, P., & Saar, S. H. 2011b, ApJ, 733, 115
Mermilliod, J.-C., Turon, C., Robichon, N., Arenou, F., & Lebreton, Y. 1997, in ESA Special Publication 402, Hipparcos—Venice '97, ed. R. M. Bonnet et al. (Paris: ESA), 643
Moraux, E., Artemenko, S., Bouvier, J., et al. 2013, A&A, 560, A13
Newton, E. R., Irwin, J., Charbonneau, D., et al. 2016, ApJ, 821, 93
Palla, F., & Stahler, S. W. 1990, ApJL, 360, L47
Pantolmos, G., & Matt, S. P. 2017, ApJ, 849, 83
Patience, J., Ghez, A. M., Reid, I. N., & Matthews, K. 2002, AJ, 123, 1570
Paxton, B., Bildsten, L., Dotter, A., et al. 2011, ApJS, 192, 3
Paxton, B., Cantiello, M., Arras, P., et al. 2013, ApJS, 208, 4
Paxton, B., Marchant, P., Schwab, J., et al. 2015, ApJS, 220, 15
Pecaut, M. J., Mamajek, E. E., & Bubar, E. J. 2012, ApJ, 746, 154
Pinsonneault, M. H., Terndrup, D. M., Hanson, R. B., & Stauffer, J. R. 2004, ApJ, 600, 946
Pognan, Q., Garraffo, C., Cohen, O., & Drake, J. J. 2018, ApJ, 856, 53
Qureshi, A., Naoz, S., & Shkolnik, E. 2018, arXiv:1802.08260
Radick, R. R., Skiff, B. A., & Lockwood, G. W. 1990, ApJ, 353, 524
Radick, R. R., Thompson, D. T., Lockwood, G. W., Duncan, D. K., & Baggett, W. E. 1987, ApJ, 321, 459
Rebull, L. M., Stauffer, J. R., Bouvier, J., et al. 2016, AJ, 152, 113
Rebull, L. M., Stauffer, J. R., Cody, A. M., et al. 2018, AJ, 155, 196
Rebull, L. M., Stauffer, J. R., Hillenbrand, L. A., et al. 2017, ApJ, 839, 92
Rebull, L. M., Wolff, S. C., & Strom, S. E. 2004, AJ, 127, 1029
Rebull, L. M., Wolff, S. C., Strom, S. E., & Makidon, R. B. 2002, AJ, 124, 546
Reiners, A., & Mohanty, S. 2012, ApJ, 746, 43
Réville, V., Brun, A. S., Matt, S. P., Strugarek, A., & Pinto, R. F. 2015, ApJ, 798, 116
Sadeghi Ardestani, L., Guillot, T., & Morel, P. 2017, MNRAS, 472, 2590
Sanz-Forcada, J., Micela, G., Ribas, I., et al. 2011, A&A, 532, A6
See, V., Jardine, M., Vidotto, A. A., et al. 2018, MNRAS, 474, 536
Skumanich, A. 1972, ApJ, 171, 565
Soderblom, D. R. 1983, ApJS, 53, 1
Spada, F., Lanzafame, A. C., Lanza, A. F., Messina, S., & Collier Cameron, A. 2011, MNRAS, 416, 447
Stahler, S. W. 1983, ApJ, 274, 822
Stauffer, J. R. 1997, MmSAI, 68, 845
van Saders, J. L., Ceillier, T., Metcalfe, T. S., et al. 2016, Natur, 529, 181
van Saders, J. L., Pinsonneault, M. H., & Barbieri, M. 2018, arXiv:1803.04971
Waite, I. A., Marsden, S. C., Carter, B. D., et al. 2015, MNRAS, 449, 8
Weber, E. J., & Davis, L., Jr. 1967, ApJ, 148, 217
Wright, N. J., Drake, J. J., Mamajek, E. E., & Henry, G. W. 2011, ApJ, 743, 48
Wu, Z.-Y., Zhou, X., Ma, J., & Du, C.-H. 2009, MNRAS, 399, 2146
Zahn, J.-P. 1977, A&A, 57, 383